

T2
3
4

MIT LIBRARIES
3 9080 02993 0127

G. C. Manning
3/19/51

V393
.R468

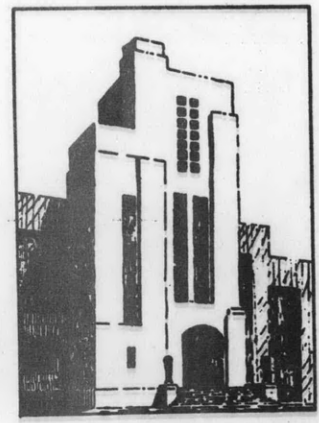
NAVY DEPARTMENT
THE DAVID W. TAYLOR MODEL BASIN
WASHINGTON 7, D.C.

**TESTS ON WAVE RESISTANCE OF IMMERSED BODIES
OF REVOLUTION**

by

[REDACTED]

G. Weinblum, H. Amsberg and W. Bock, Berlin



MASS. INST. OF TECHNOLOGY
JUL 13 1976
BARKER ENGINEERING LIBRARY

September 1950

Translation 234

TESTS ON WAVE RESISTANCE OF IMMERSSED BODIES
OF REVOLUTION
(VERSUCHE ÜBER DEN WELLENWIDERSTAND GETAUCHTER
ROTATIONSKÖRPER)

by

G. Weinblum, H. Amsberg and W. Bock, Berlin

Mitteilungen der Preussischen Versuchsanstalt
für Wasserbau und Schiffbau, Berlin, 1936

Figures 17-20 added by M. Gertler

Translated by G. Weinblum and R. Widmer

NOTATION

$B = 2b$	Diameter of body
$L = 2a$	Length of body
C_t	Total resistance coefficient
C_f	Frictional resistance coefficient
C_r	Residual resistance coefficient
C_R	Wave resistance coefficient
$F = \frac{v}{\sqrt{gL}}$	Froude number
F_k	Hypothetical critical value of F
$F' = \frac{v}{\sqrt{gf}}$	Froude number referred to depth of immersion
$F'_k = 1$	Critical value of F'
R	Wave resistance
R_t	Total resistance
$a = L/2$	Half length of body
$b = B/2$	Radius of body
f	Depth of immersion
t	Taylor's tangent value
v	Speed of advance
v_k	Critical speed of advance
λ	Wave length
ξ	Dimensionless longitudinal coordinate
$\phi = C_p$	Prismatic coefficient
$\psi = f/a$	Immersion parameter

TESTS ON WAVE RESISTANCE OF IMMERSED BODIES OF REVOLUTION

OBJECT OF INVESTIGATION

It is known that the airplane and the submarine submerged at great depth present identical problems from a hydrodynamic standpoint; their motions are investigated by methods developed for bodies moving in an unbounded medium.

The normal ship floating on the water surface is hydrodynamically a more complicated problem than the airplane and the submarine and considerable difficulties can arise when the laws valid for bodies moving in an unbounded liquid are applied directly to ships. Figure 1 shows a body which moves fully submerged but is too near to the surface to assume practically infinite submergence. This applies, for example, to torpedoes and, under special conditions, to submarines. In such cases the wave resistance will not disappear. The problem illustrated by Figure 1 has also some bearing on an important experiment: In determining the "separation" resistance of submerged bodies, the question arises, how far the model should be submerged to justify neglecting of the wave resistance. This problem was not considered at times and consequently, errors were committed which invalidate some frequently used results.

More exhaustive theoretical studies, showing a series of remarkable results¹ induced the first author to approach the subject. Tests were made at the "Preussische Versuchsanstalt für Wasserbau und Schiffbau" Berlin with the idea to check calculated results representing the wave resistance as a function of the form of the body, depth of immersion and Froude number. It is not intended to discuss in this report technical applications, but only to explain some physical phenomena.

RESULTS OF THEORETICAL REASONING

The choice of simple shapes such as bodies of revolution appeared to be necessary from a practical as well as theoretical viewpoint. The basic principles were published by Havelock² in a series of papers, from which a wave resistance formula for bodies of revolution can be immediately derived. Assumptions on which the theory is based are essential: The most important limitation consists in the fact that the depth of immersion f is large enough compared with the diameter of the body $2b$. Havelock has shown that in the case of a circular cylinder (generating line horizontal, normal to the direction of motion) at $f = 2b$ the difference between the first approximation

¹Numbers indicate references on page 9.

and a second one is quite considerable; however, it can be expected that elongated bodies of revolution present more favorable conditions. Within this paper even such a low value as $f = b$ is admitted with the purpose of obtaining a practical limit for the application of the theory.

We refer to a few results mentioned in Reference 1. There optimum contours of bodies of revolution have been calculated to a first approximation for different Froude numbers and depths of immersion. Among other results, it was found that the smallest wave resistance ($f = 2b$) corresponds

- 1) For $F = \frac{v}{\sqrt{gL}} = 0.408$ to a very full body
- 2) For $F = 0.354$ to a body somewhat fuller than an ellipsoid, and
- 3) For smaller F to a fine body with hollow ends of the sectional area curve.

These results seemed to be so interesting that they were used as a starting point for the tests in question. Unfortunately the optimum models could not be made, but accidentally, two bodies of revolution were available, left over from a test made by W. Amtsberg.³ The first of these models (Model No. 1257) was relatively full, the second model (Model No. 1242) had a small prismatic coefficient and a tangent value of the sectional area curve $t = 0$. An ellipsoid of revolution (Model No. 1286) was built anew as a third model. The contours of the bodies of revolution and the sectional area curves are shown in Figure 2. The calculated resistance for $f = 2b$ and $f = 4b$ are shown in Figure 3; it is emphasized that the shape of the curves can be somewhat arbitrary, as the number of calculated points is not sufficient. However, the accuracy is satisfactory for the requirements under consideration.

The most important data on models are summarized in Table 1.

For further details, reference is made to the paper by Amtsberg.³

The computation of the wave resistance of bodies of revolution submerged at finite depth is similar in various respects to the procedure used for the wave resistance of surface ships. Many simplifications are given by axial symmetry; new complications arise by the additional dependency upon the depth of immersion. Results of previous and present investigations are summarized as follows:

1. The wave resistance R of a body of revolution immersed at finite depth is a function of the equation of the surface, the depth of immersion and the velocity; the last two values are written in a non-dimensional form:

$$\frac{f}{a} = \psi \quad \text{and} \quad \frac{v}{\sqrt{gL}} = \frac{v}{\sqrt{2ga}} = F$$

TABLE 1

Principal Dimensions L and B are the Same for all Models; $\frac{L}{B} = 8$

Model Number	Length L = 2a m	Diameter B = 2b m	Volume V m ³	Wetted Surface m ²	Prismatic Coefficient $\phi = \frac{\delta}{\beta} = C_p$	Initial Value t of the Tangent of the Sectional Area Curve	Equation for the Doublet Distribution	Fullness of the Doublet Distri- bution
1242	} 4	} 0.5	0.429	4.26	0.546	0	$1 - 2\xi^2 + \xi^4$	0.533
1257			0.628	5.46	0.800	0	$1 - 3.0825 \xi^8 + 0.165 \xi^{10} - 1.9175 \xi^{12}$	0.820
1286			0.524	4.94	0.667	2	$1 - \xi^2$	0.667
1242 + 1257			0.528	4.86	0.673	0		

2. Within the limits of theory (radius b small compared to the depth of immersion) the wave resistance R , independently of the Froude number, is found to be closely proportional to the fourth power of the radius of the body, $R \sim b^4$. For surface ships according to Michell's theory,⁴ R is approximately proportional to B^2H^2 only at very high F ; the exponent of H is considerably smaller than 2 at medium and small F .

3. The humps and hollows of the resistance curves are even more pronounced than for surface ships. The ordinates of the resistance curve outside of the first hump decrease quickly when the depth of immersion is increased. For example, the wave resistance of Model No. 1242 (see Figure 3) attains a considerable value at $f = 2b$ within the range of the first hump, whereas the second hump can be nearly neglected. The very pronounced hollows and humps in the resistance curve especially in fuller forms, explain why forms of least resistance vary more rapidly with Froude number than for surface ships. While in surface ships the optimum of the prismatic coefficient increases almost monotonically within the range $0.3 \leq F \leq 0.50$ and then remains approximately constant, ($\phi \cong 0.64$) there exists for deeply immersed bodies a region between $F \cong 0.37$ and 0.45 , where extremely high prismatics present great advantages. This difficult behavior can be formally explained by the presence of one function in the integrand of the resistance.

Due to the unusually large variety of possible forms, results should be generalized with caution, a fact which will have to be considered specially later when discussing resistance curves.

4. Considerable interest is connected with the problem of the limiting depth of immersion f_0 , below which the wave resistance can be practically neglected. In the first place, this value has to be a function of the length of the free wave $\lambda = \frac{2\pi v^2}{g}$ corresponding to the velocity v . Expressed in terms of the Froude number, $\frac{f_0}{L} = 2\pi F^2$.

The amplitude of a free two-dimensional wave is negligible at $f = 0.75\lambda$, its value being about 1 percent of the surface amplitude. Therefore, it can be expected that no noticeable wave resistance occurs at a Froude number of 0.30 when $\frac{f}{L} \cong 0.4$. This is actually even the case for the fullest model, No. 1257. Hence, the free wavelength can be used as an approximate criteria for f_0 . However, if a more accurate limit is desired, generally the form of the body must be considered. For Model No. 1242, for example, an immersion of $f = 4b$ at F below ~ 0.31 is equivalent to practically infinite immersion.

5. From investigations on the circular cylinder and the sphere $v_k = \sqrt{fg}$ appears to be the critical velocity producing the maximum resistance. With elongated bodies of revolution, however, this value is not decisive. The Froude number based on f

$$F' = \frac{v}{\sqrt{gf}} \text{ becomes}$$

$$F'_k = \frac{v_k}{\sqrt{fg}} = 1$$

for $v_k = \sqrt{fg}$. The normal Froude number with $L = 2a$ is in this case

$$F_k = \frac{v_k}{2ag} = \frac{v_k}{\sqrt{fg} \sqrt{\frac{2a}{f}}} = \sqrt{\frac{f}{2a}}$$

Using the table

$\frac{f}{b} =$	1	2	4
$\frac{f}{2a} = \frac{\psi}{2}$	1/16	1/8	1/4
F_k	0.25	0.35	0.50

a pronounced maximum could be expected for all bodies at $F_k = 0.35$ and a depth of immersion $f = 2b$. It can be seen from the curves in Figure 3 that such a maximum does not exist; the speed $v = \sqrt{fg}$ does not indicate a peculiar point in the wave resistance curve of elongated bodies. The longitudinal distribution of displacement becomes decisive. Therefore, one must be cautious when generalizing results based on such simple forms as spheres and cylinders.

6. Curves of wave resistance R for $F = \text{constant}$ are shown in Figure 4 plotted on f/b as abscissas. Because of the small number of points the form of the curves is somewhat arbitrary. However, in agreement with Points 3 and 4 the following conclusions can be derived. The wave resistance decreases rapidly with increasing depth of immersion especially for lower Froude numbers (compare e.g. the intersecting curves for $F = 0.408$ and $F = 0.316$ Model No. 1257). Occasionally, these investigations should be extended to higher immersions f/b .

7. Figure 3 shows how basically different the three models behave at identical depths of immersion ($f = 2b$ and $f = 4b$). The first hump is very pronounced in all cases, while the second is only pronounced in Model No. 1257, and is hardly noticeable in Model No. 1242. Although the models used differ widely from optimum forms obtained by calculation, the conclusions as to the best prismatic coefficients (see page 2) are supported by our experiments: $F = 0.408$ —optimum model 1257, $F = 0.354$ —optimum model 1286, $F = 0.316$ —~~below~~ optimum model 1242.

TEST RESULTS

The experimental methods are described in a paper by Graff.⁵ According to the given depth of immersion, either one of the two apparatuses developed at the Berlin Tank was used. Corresponding calculations, the values $f = b, 2b, 4b$, were chosen for all models. In addition, tests at the depth of immersion $f = 6b$ were available³ for the Models No. 1242 and 1257; this immersion can be considered as infinitely large for medium Froude numbers. The ellipsoid was also towed at a depth of $f = 3b$, and to finish the picture, the series was completed by tests of all models on the surface. In this case, the draft at the middle section was $T = b$ and the displaced volume was one-half of the entire volume of the body of revolution.

The results are plotted as absolute values and as coefficients of the total resistance. At first, the absolute values will be discussed; see Figures 5, 6, and 7. In addition to the experimental points, for comparison, the sum of the calculated wave resistance and the viscous resistance measured at infinite depth of immersion has been plotted. The viscous resistance coincides with the curve $f = 6b$ for mean Froude numbers. There is a considerable phase lag between the theoretically and the experimentally determined curves. We treat the case $f = 2b$. In the range of the first hump, the phase displacement agrees with our experiences with surface ships. However, within the region of the second hump the experimental curve precedes the theoretical or, otherwise expressed, the theory lags contrary to results found for surface ships. Havelock gave a plausible explanation for the latter case, pointing out that the wake increases the wave-making length and, therefore, actually decreases the Froude number. First, the explanation is attempted that the small depth of immersion equal to one diameter caused the peculiar phase displacement. This fact is also sustained by the different position of the second hump at a larger depth of immersion $f = 4b$, and by the good agreement found in this case between measurement and calculation—as far as such an agreement can still be stated for so small values of the wave resistance. However, it is not impossible, that in view of the observations just mentioned on Model No. 1257 which are apparently also confirmed by measurements of the ellipsoid model No. 1286, it will be necessary under certain conditions to check Havelock's hypothesis.

The trace of the measured-wave-resistance curve agrees satisfactorily with theory in spite of the phase lag, as soon as $f = 2b$, i.e., if theory is really applicable. However, even in the case $f = b$, the calculation fails completely only for the full model No. 1257; for the other two models the order of magnitude is reproduced correctly. The figures show how the merit of different bodies varies with Froude numbers, entirely in agreement with theoretical deductions. For example, at $F = 0.36$, the total resistance of the finest model No. 1242 is larger than the total resistance of Model No. 1257 although the latter has a much higher displacement. From theoretical reasoning it follows that this relationship is reversed at higher Froude numbers ($F \geq \sim 0.45$, see Figure 3). Experimental results for this case are not

available since the towing velocity was restricted by the relatively large size of the models. Although it is desirable to attain much higher Froude numbers this is not absolutely necessary for the present purpose since it can be deduced, from the results so far obtained, that the theory reproduces facts which are basically correct.

The reason for the excessive second hump in the resistance curve of the fullest model No. 1257 is obviously the high prismatic coefficient. The same explanation applies to a model test by Graff.⁵

The curves of the coefficients of the total resistance $C_t = \frac{R_t}{\rho/2v^2S}$ (see Figures 8 to 13) show the oscillating character still more clearly. The selection of the wetted surface can be justified by the fact that at large depths of immersion C_t differs very little from the friction coefficient C_f , although the wetted surface is by no means characteristic for the wave-resistance. The ratio $S/v^{2/3}$ does not differ too much for the three models.

Figures 8 to 12 show the measured resistance values for $f = 0$, and for the asymmetrical combination 1242 + 1257 (or 1257 + 1242 when run astern) for which no elaborate theoretical computations have been made.

The C_t curves show some surprising results. Let us begin with Figure 8, Model No. 1242. On the surface this body is not particularly unfavorable. Although the coefficient $C_{t(f=0)}$ increases at first contrary to the fully submerged condition $C_{t(f=2b)}$, at Froude numbers of about 0.33, $C_{t(f=0)}$ becomes more favorable than $C_{t(f=2b)}$ i.e., the resistance of the surface ship (displacement $\frac{V}{2}$) is less than one-half the resistance of the body of revolution (immersed to $f = 2b$) having the volume V . For the immersion $f = b$, higher $C_{t(f=b)}$ are obtained than $C_{t(f=0)}$ over the entire towing range. At first, this result seems to contradict completely the good rule of thumb; by increasing the immersion of a given volume the wave resistance is reduced. However, this paradox is only apparent, as the mentioned rule applies only to a constant volume. By doubling the displacement of surface ships, keeping the shape of the area curve and $L = \text{constant}$, we increase the wave resistance more than twice, actually four times at high Froude numbers.

We note:

$$V_{(f=0)} : V_{(f=b)} = \frac{1}{2} \qquad S_{(f=0)} : S_{(f=b)} = \frac{1}{2}$$

In the limiting case, of extreme Froude numbers it follows from theory that

$$R_{(f=0)} : R_{(f=b)} \cong \frac{1}{4}$$

and the ratio of the coefficients of the wave resistance

$$C_{R(f=0)} : C_{R(f=b)} = \frac{1}{2}$$

Only if the coefficient $C_{R(f=0)}$ were smaller than $1/2 C_{R(f=b)}$ would a real paradox exist. Actually $C_{R(f=0)}$ always remains larger than $1/2 C_{R(f=b)}$.

The results for the full model No. 1257 are not less instructive (see Figure 9). On this full model we can prove the mentioned result deduced theoretically, that the optimum sectional area curves with respect to wave making may be totally different for a surface ship and for an immersed body of revolution. While the shape of the body No. 1257 is very unfavorable when moving on the surface, especially for medium Froude numbers (0.30), it becomes advantageous when totally submerged. The values $C_{R(f=b)}$ at $F \approx 0.35$ amounts to only about 40 percent of $C_{R(f=0)}$ and $C_{R(f=2b)}$ is less than $0.05 C_{R(f=0)}$. The curves of the coefficients $C_{t(f=b)}$ and $C_{t(f=2b)}$ still show the "third hump." For the ellipsoid (Figure 10) high values of the coefficient $C_{R(f=0)}$ are obtained at lower speeds, probably due to the high tangent value $t = 2$ of the sectional area curve. H. Amsberg has suggested towing tests on the surface with fixed trim, as in the immersed condition. The C_t curve for the ellipsoid obtained in this way lies considerably below the curve shown in Figure 10. Because of some doubts as to its accuracy this curve has not been reproduced. It is important to continue these investigations.

Finally, reference is made to the combined model No. 1242 + No. 1257, the forebody of which represents half of the model No. 1242 and the afterbody of which represents half of the model No. 1257. The prismatic coefficient of the combined body is nearly equal to the prismatic coefficient of the ellipsoid. Neglecting the difference in t values, similar $C_{R(f=2b)}$ values as for the ellipsoid should be expected, increased by an amount due to the strong asymmetry of the fore- and afterbody. Theoretically, the coefficients $C_{R(f=2b)} \approx C_{f(f=2b)} - C_{f(f=6b)}$ should be the same when moving forward (see Figure 11) and astern (see Figure 12), if the viscosity can be neglected.

Figures 11 and 12 furnish a nice confirmation of this fundamental theoretical conclusion.

For a better survey, the coefficients of all three models are summarized once more in Figure 13. Figures 17 - 20 prepared by Mr. Gertler present the residual-resistance coefficients.

As only a few reports of towing tests with bodies of revolution on the surface have been published, several photographs are shown in Figure 14. The reason for superiority of the model No. 1242 at smaller and medium

velocities over the other models can easily be seen; likewise, the heavy trim at 2.5 m/sec indicates a considerable increase of resistance. Model 1257 is characterized by its large bow wave. The towing apparatus can easily be recognized.

Turning to Figure 15 (depth of immersion $f = b$), we remark that the back of the models is already set free at relatively small velocities. Therefore, the wetted surface as a reference magnitude has only a conventional value.

Finally reference is made to Figure 16 ($f = 2b$) which shows how considerable the wave formation is.

SUMMARY

From the theory of wave resistance various deductions can be made on the resistance of bodies of revolution immersed at finite depth; especially, favorable "optimum" forms can be developed for given Froude numbers.

By testing three models it is shown that theoretical results agree well, qualitatively and even quantitatively with the experimental results, if a "phase displacement" is ignored. The theory can be used up to minimum immersions of $f = 2b$ for a length/diameter ratio $L : B = a : b = 8$; for a first orientation even $f = b$ can be admitted as long as full and short bodies are excluded.

REFERENCES

1. Weinblum, G., "Rotationskorpern geringsten Wellewilderstands (Bodies of Revolution with Minimum Wave Resistance) Ingenieur Archiv VII (1936) p. 104.
2. Havelock, Proc. Royal Society, 1919, 1931, 1932.
3. Amtsberg, H., "Untersuchungen uber die Form Abhaensigkeit des Reibungswiderstands" (Investigations on the Dependence of Frictional Resistance on Form), Jahrbuch Schiffbaut, Ges.
4. Michell, T., Phil. Magazine, London, 1898.
5. Graff, W., "Untersuchungen uber den Abloesungswiderstand Volliger Schiffsformen" (Investigations on Separation Resistance of Full Ship's Forms) Jahrbuch Schiffbaut, Ges. Vol. 35, 1934.

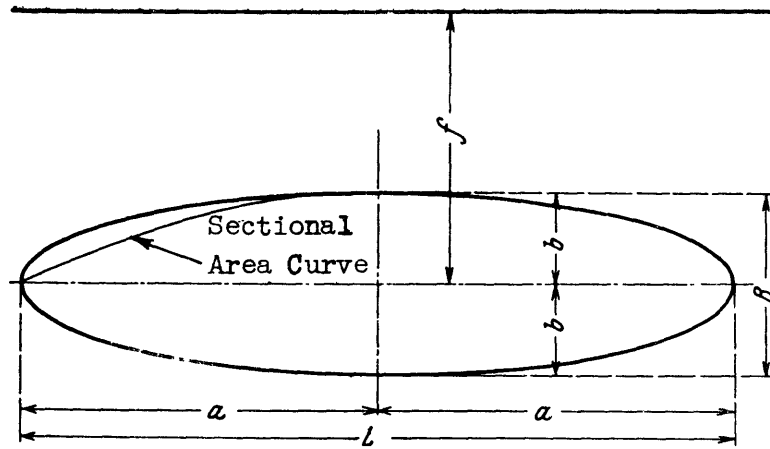


Figure 1 - Bodies of Revolution Immersed to a Finite Depth f

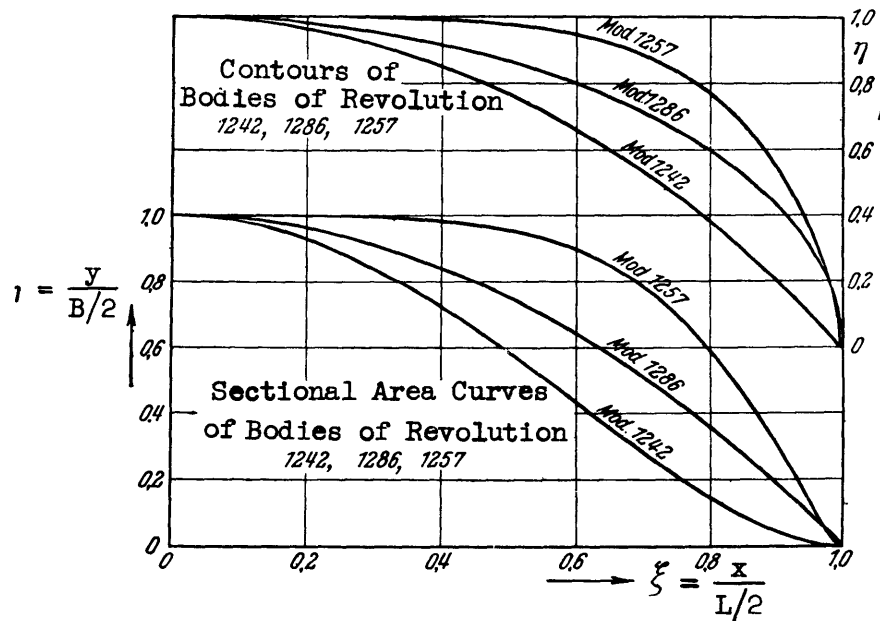


Figure 2 - Contours and Sectional Area Curves of Investigated Models

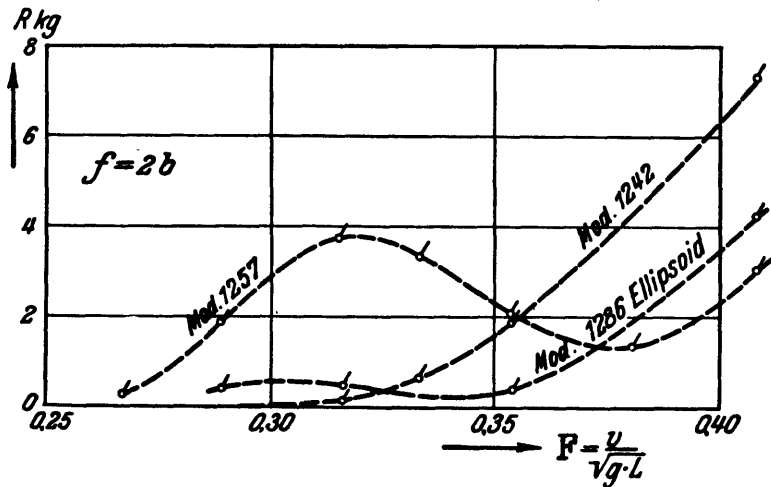
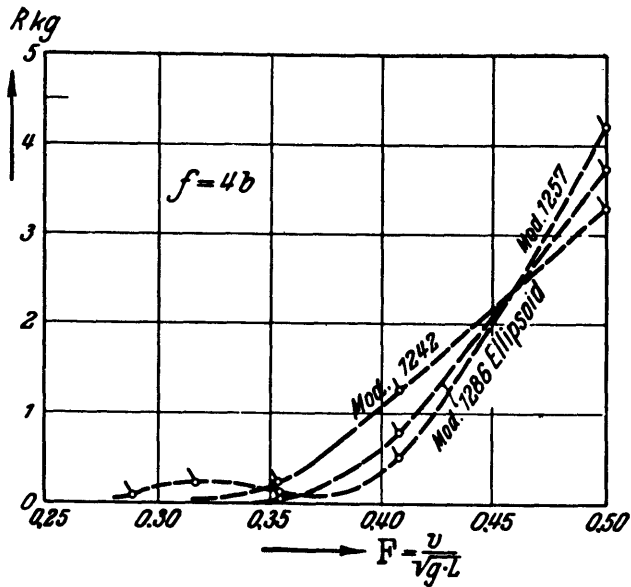


Figure 3 - Calculated Wave Resistances;
 Depths of Immersion $f = 2b$ and $4b$

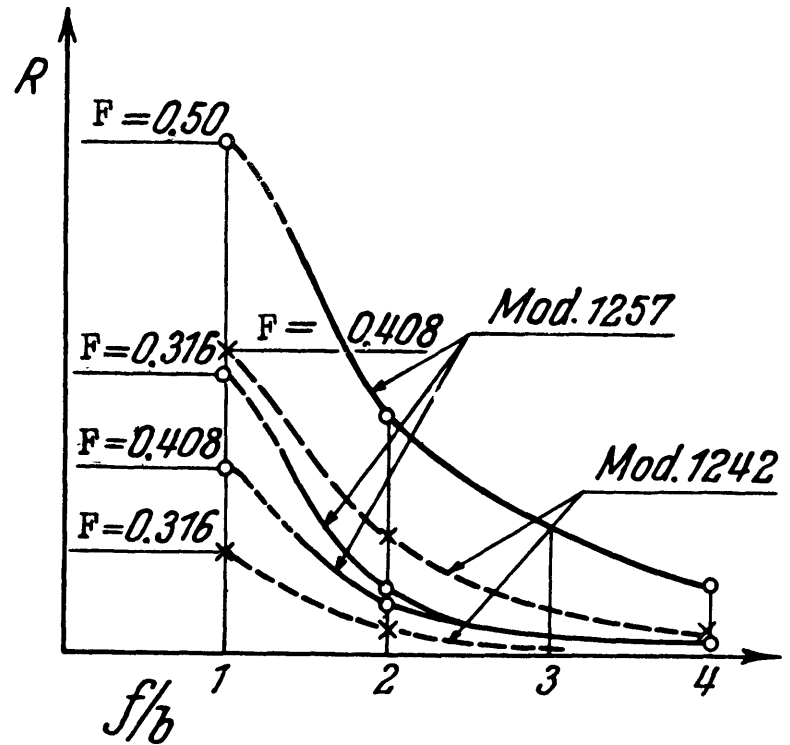


Figure 4 - Calculated Wave Resistances
 as a Function of f/b for
 $F = v/\sqrt{gL} = \text{Constant}$

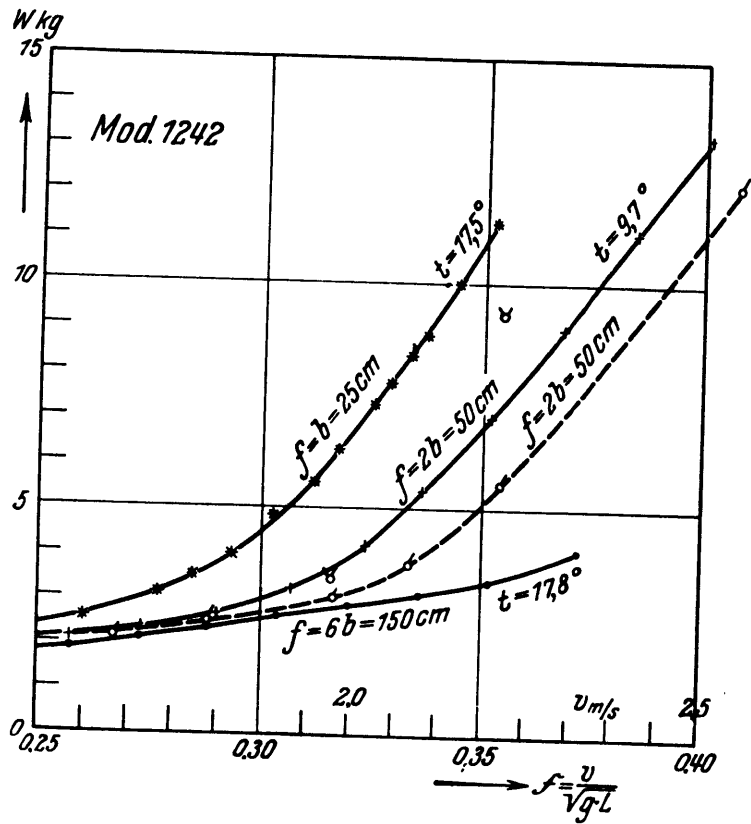


Figure 5 - Total Resistance of Model 1242. ——— Measured
 - - - Sum of Frictional Resistance and Calculated Wave Resistance,
 \circ $f = 2b$, \ast $f = b$

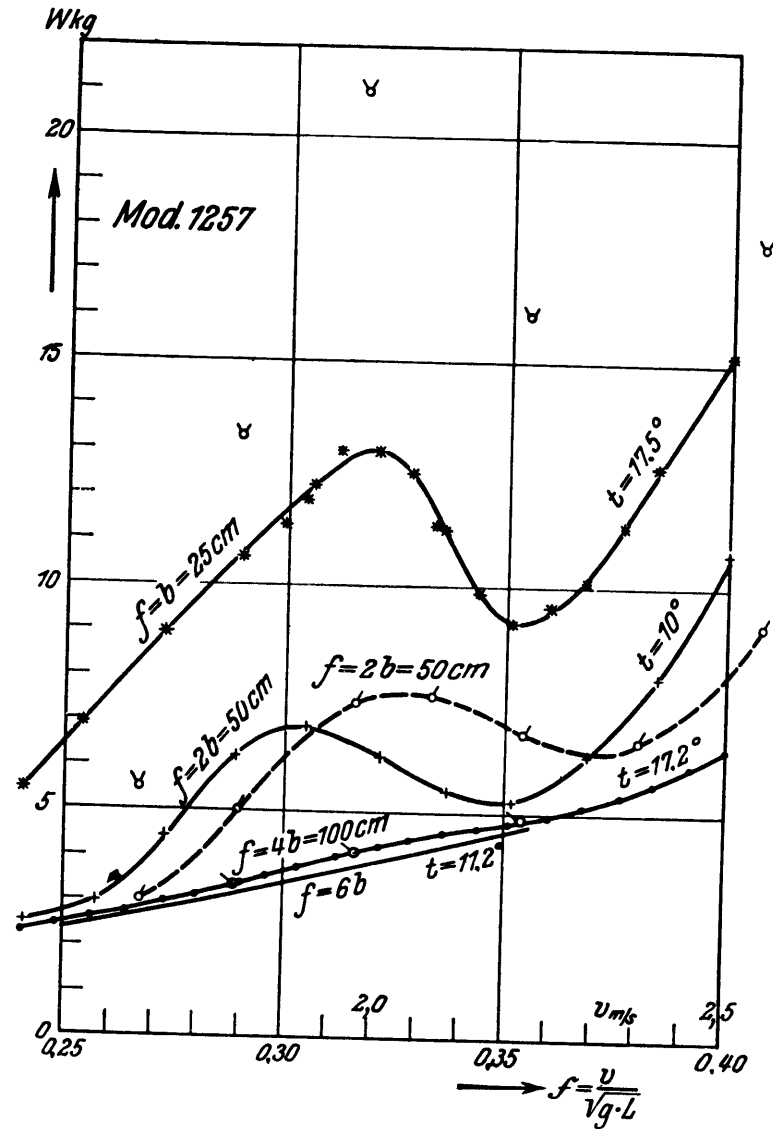


Figure 6 - Total Resistance of Model 1257. Symbols are the same as in Figure 5 and \circ is the symbol for $f = 4b$

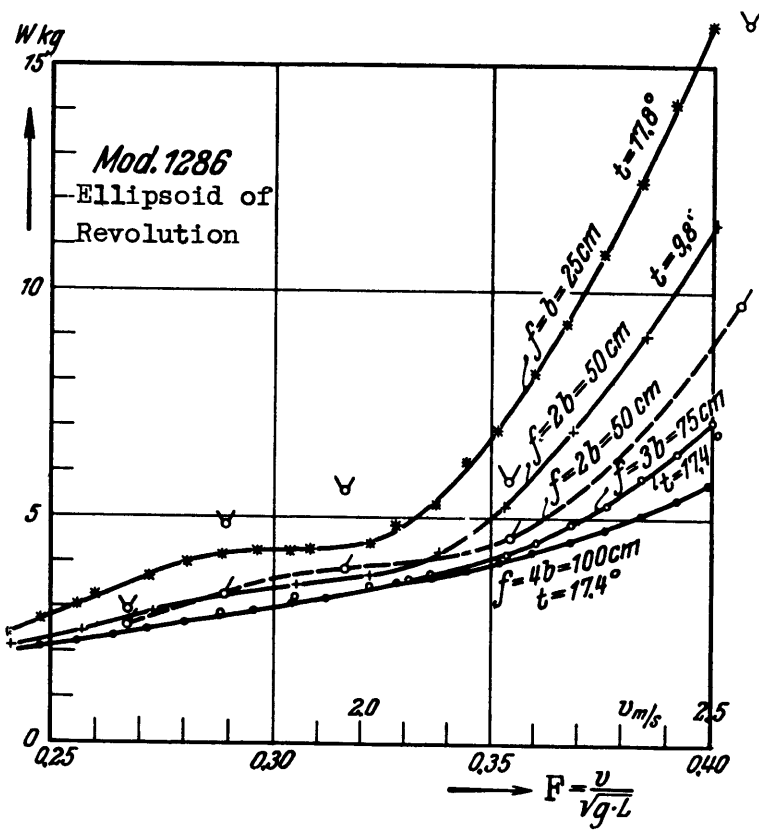


Figure 7 - Total Resistance of Model 1286 (Ellipsoid)

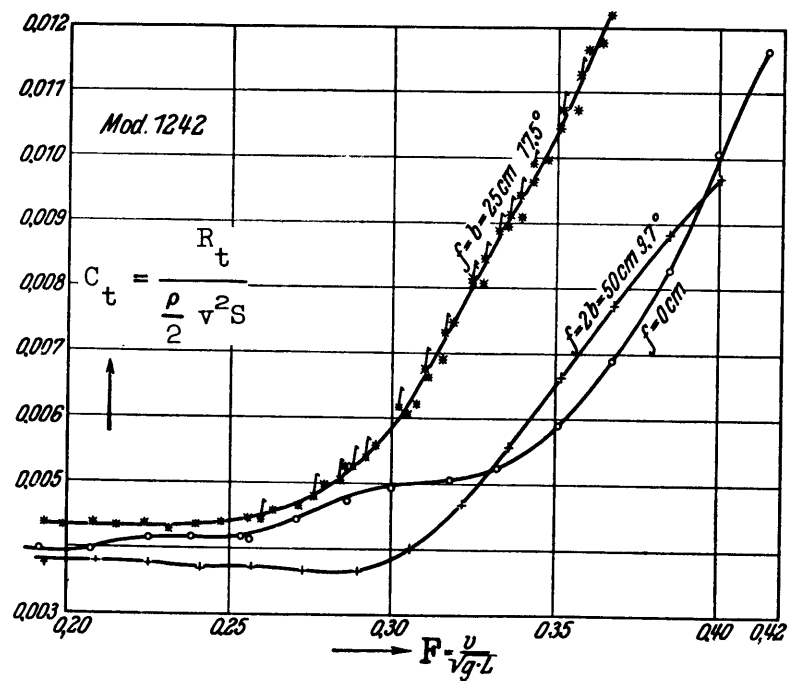


Figure 8 - Coefficients of Total Resistance of Model 1242

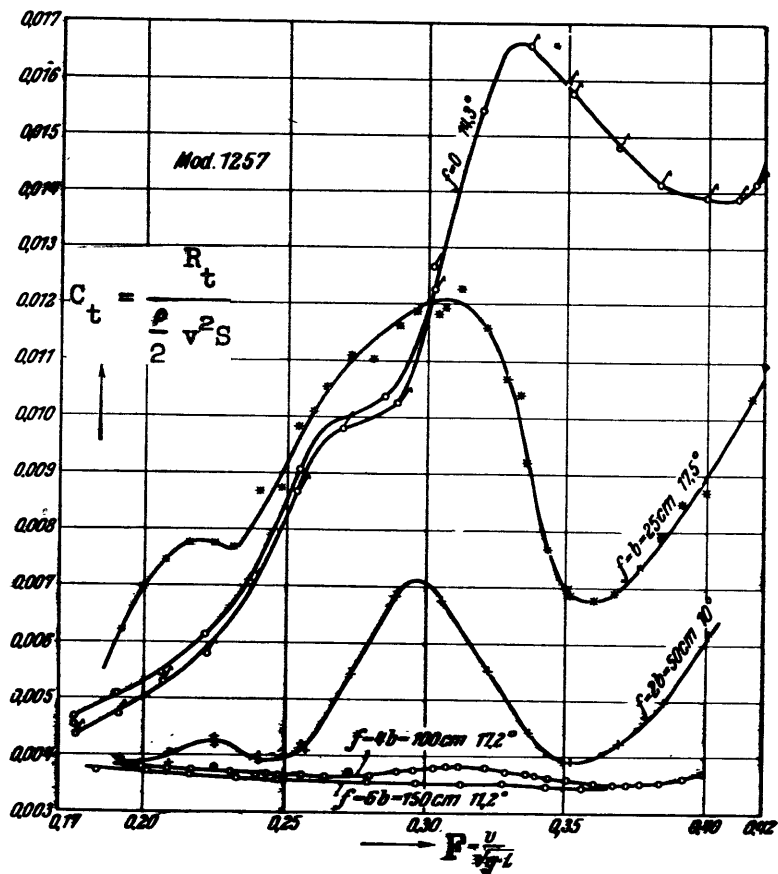


Figure 9 - Coefficients of Total Resistance of Model 1257

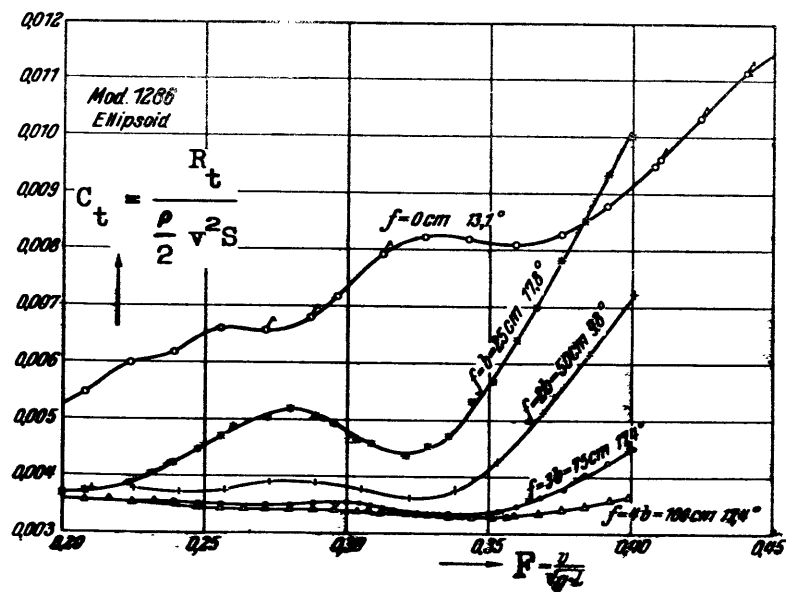


Figure 10 - Coefficients of Total Resistance of Model 1286

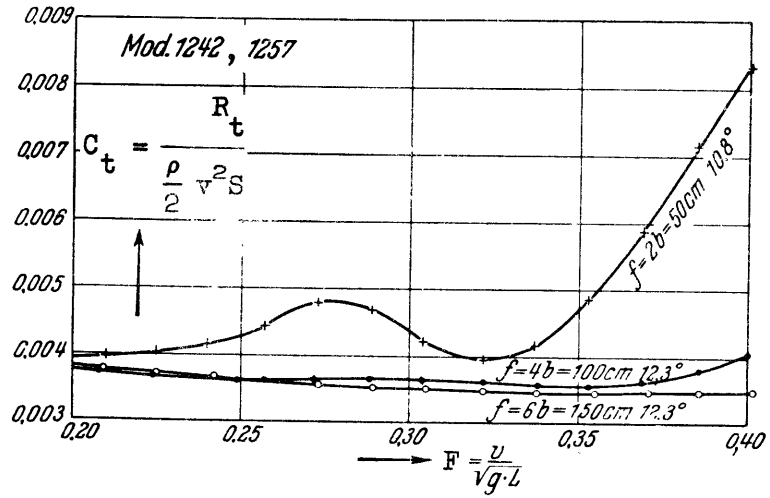


Figure 11 - Coefficients of Total Resistance of Models 1242 and 1257

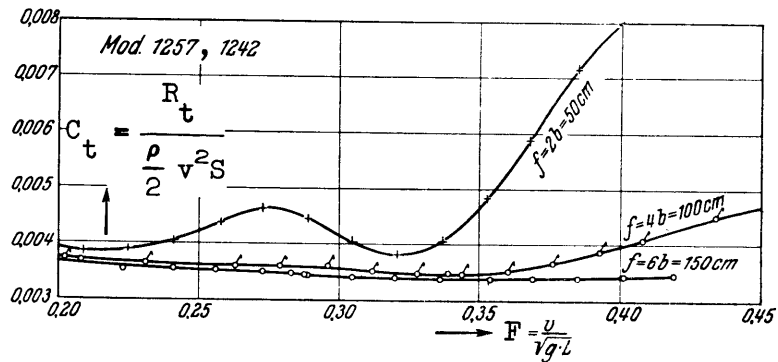


Figure 12 - Coefficients of Total Resistance of Models 1257 and 1242

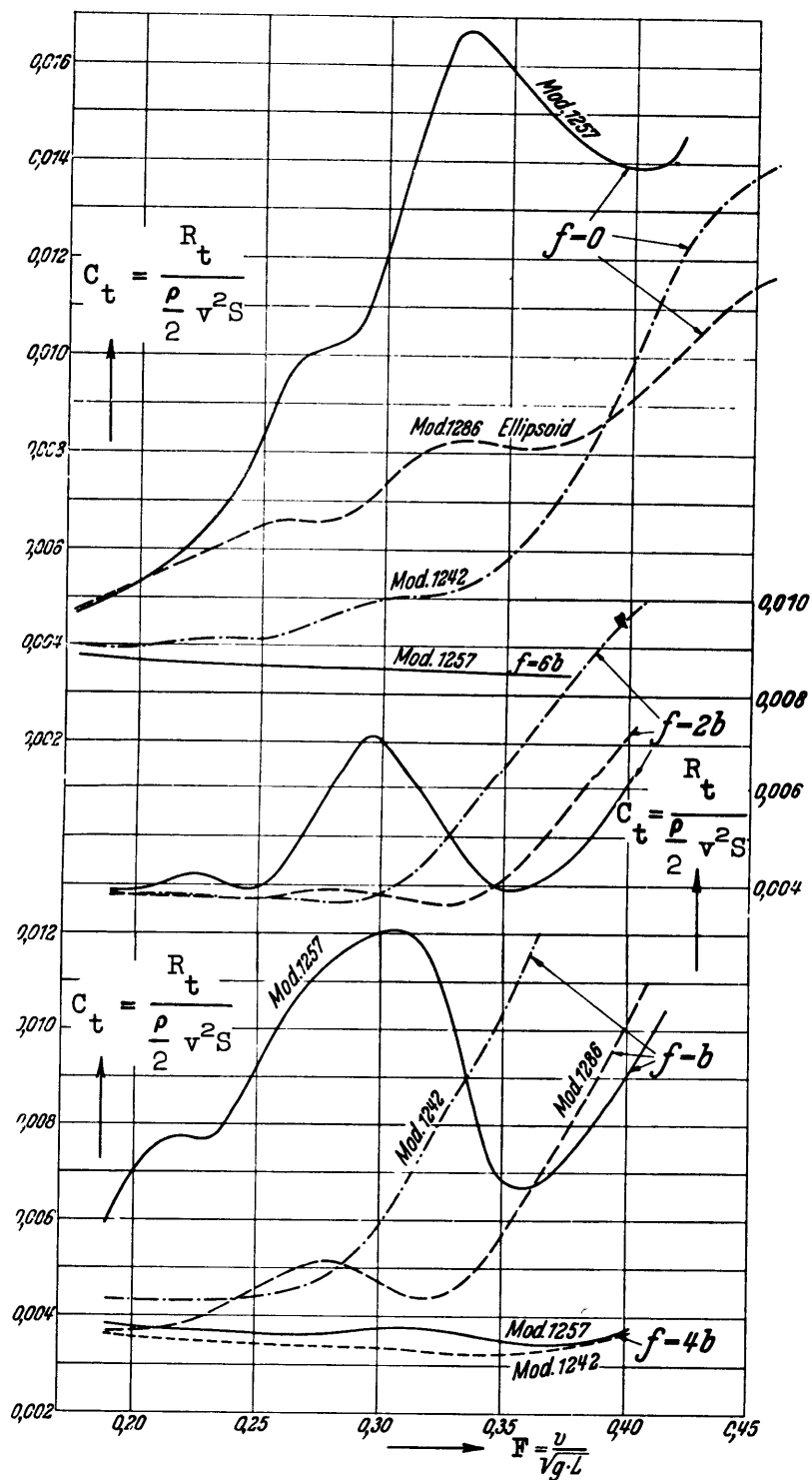
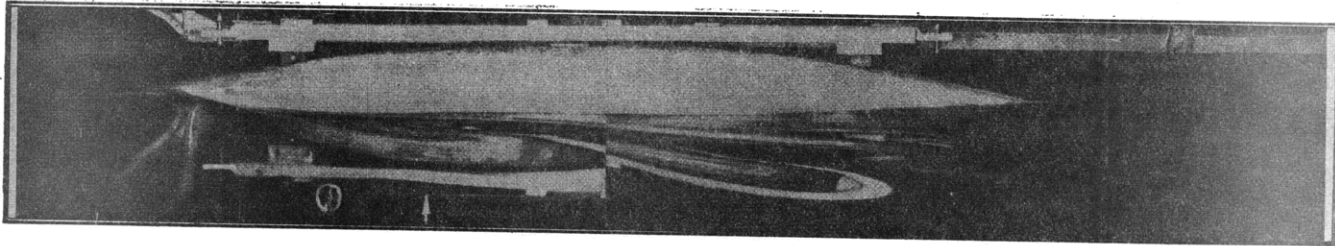
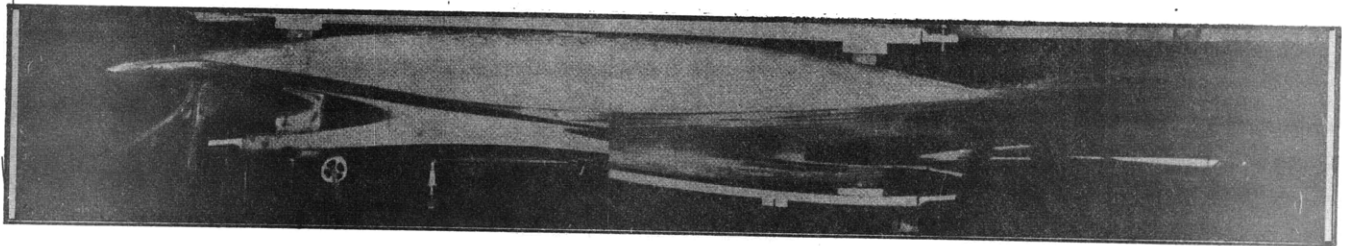


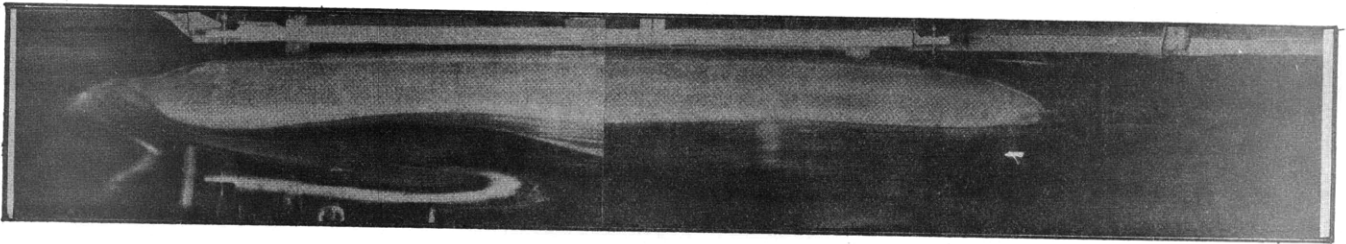
Figure 13 - Coefficients of Total Resistance of Models 1242, 1257, and 1286



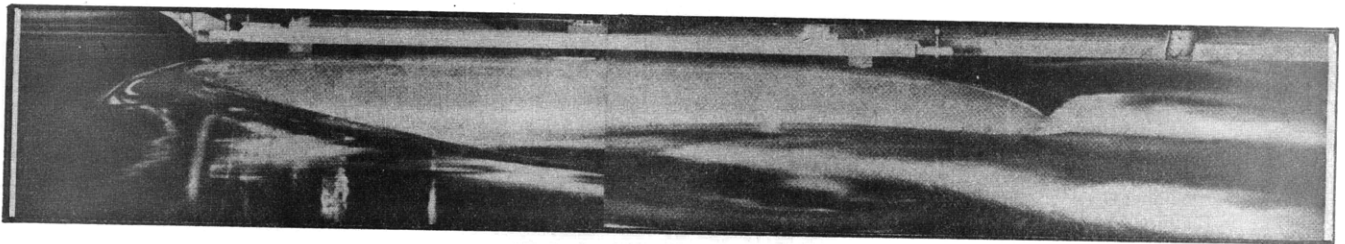
Model 1242, $F = 0.256$



Model 1242, $F = 0.40$

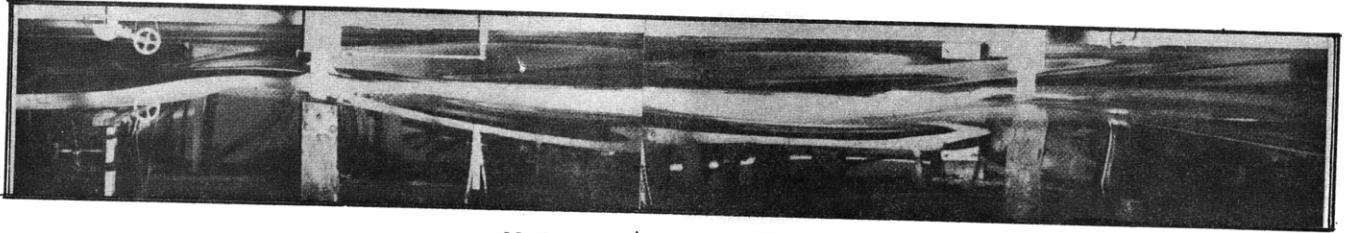
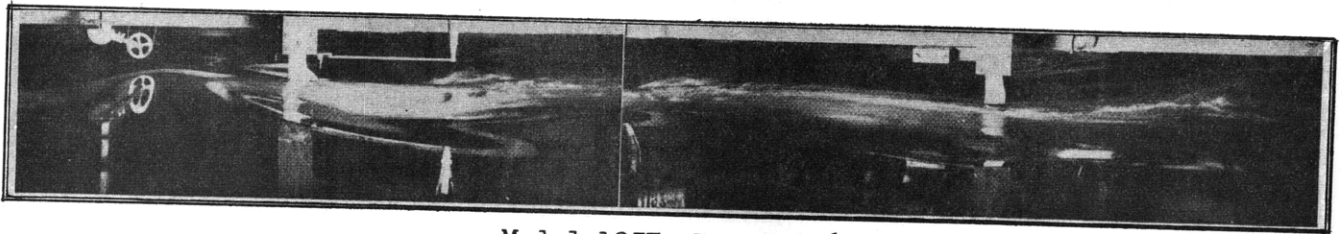
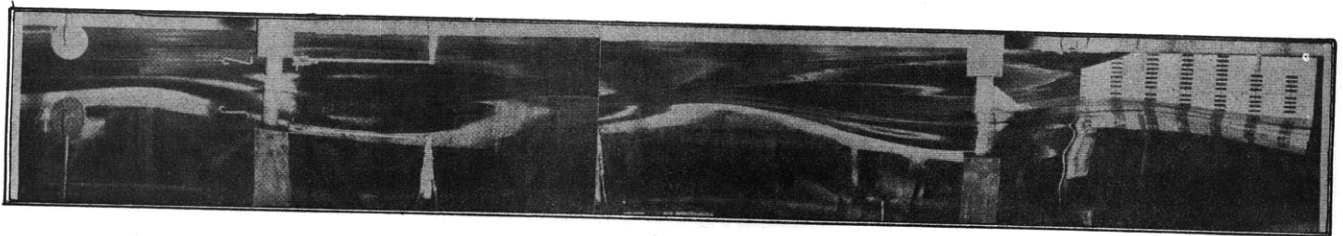


Model 1257, $F = 0.256$



Model 1257, $F = 0.40$

Figure 14 - Wave Photographs of Models 1242 and 1257, $f = 0$

Model 1242, $F = 0.256$ Model 1257, $F = 0.256$ Figure 15 - Wave Photographs of Models 1242 and 1257, $f = b$ Figure 16 - Wave Photographs of Models 1242 and 1257, $f = 2b$

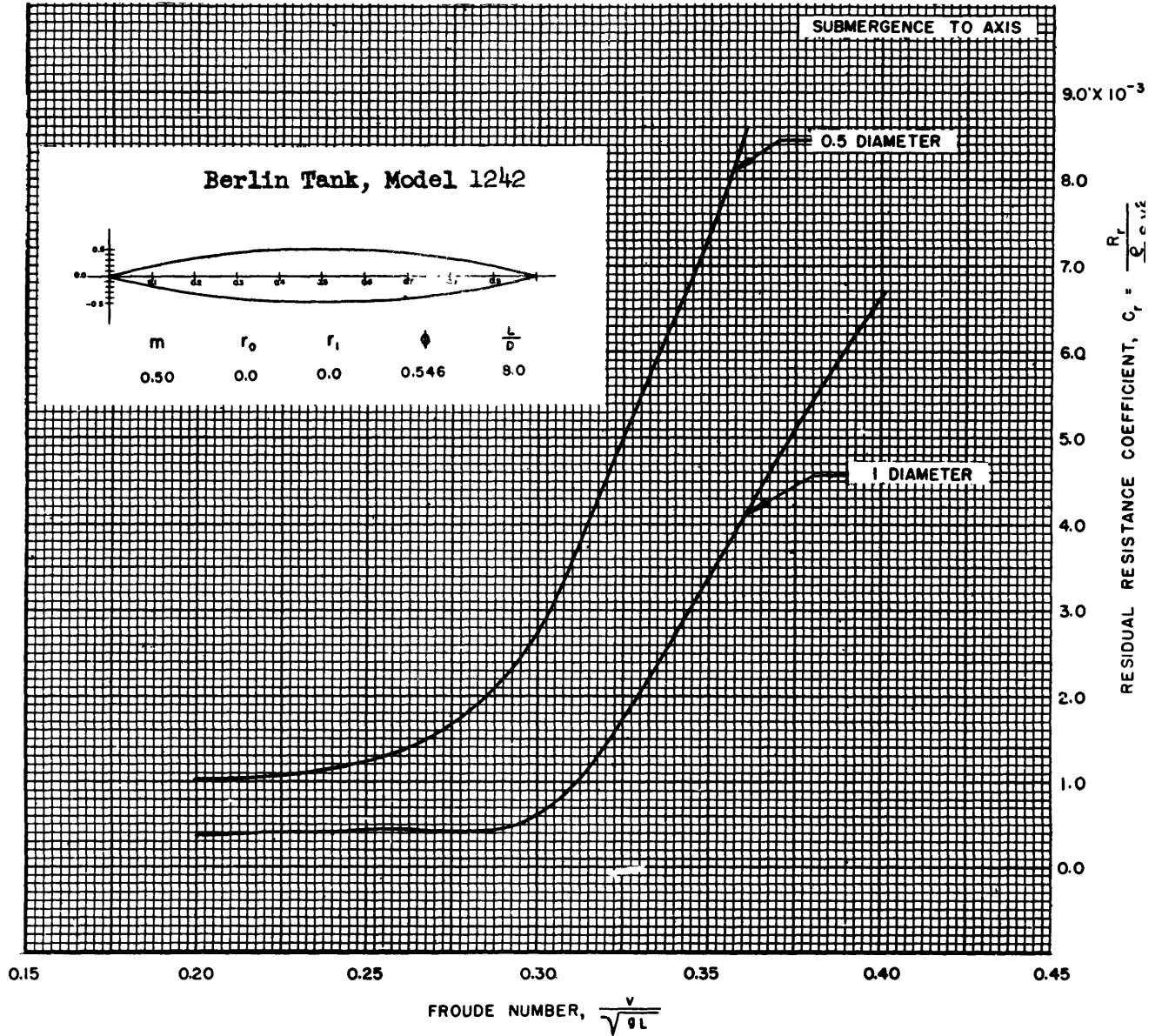


Figure 17 - Residual-Resistance Coefficient versus Froude Number for Model 1242

(The values were obtained by subtracting the Schoenherr frictional-resistance coefficients from the total-resistance coefficients of Figure 8.)

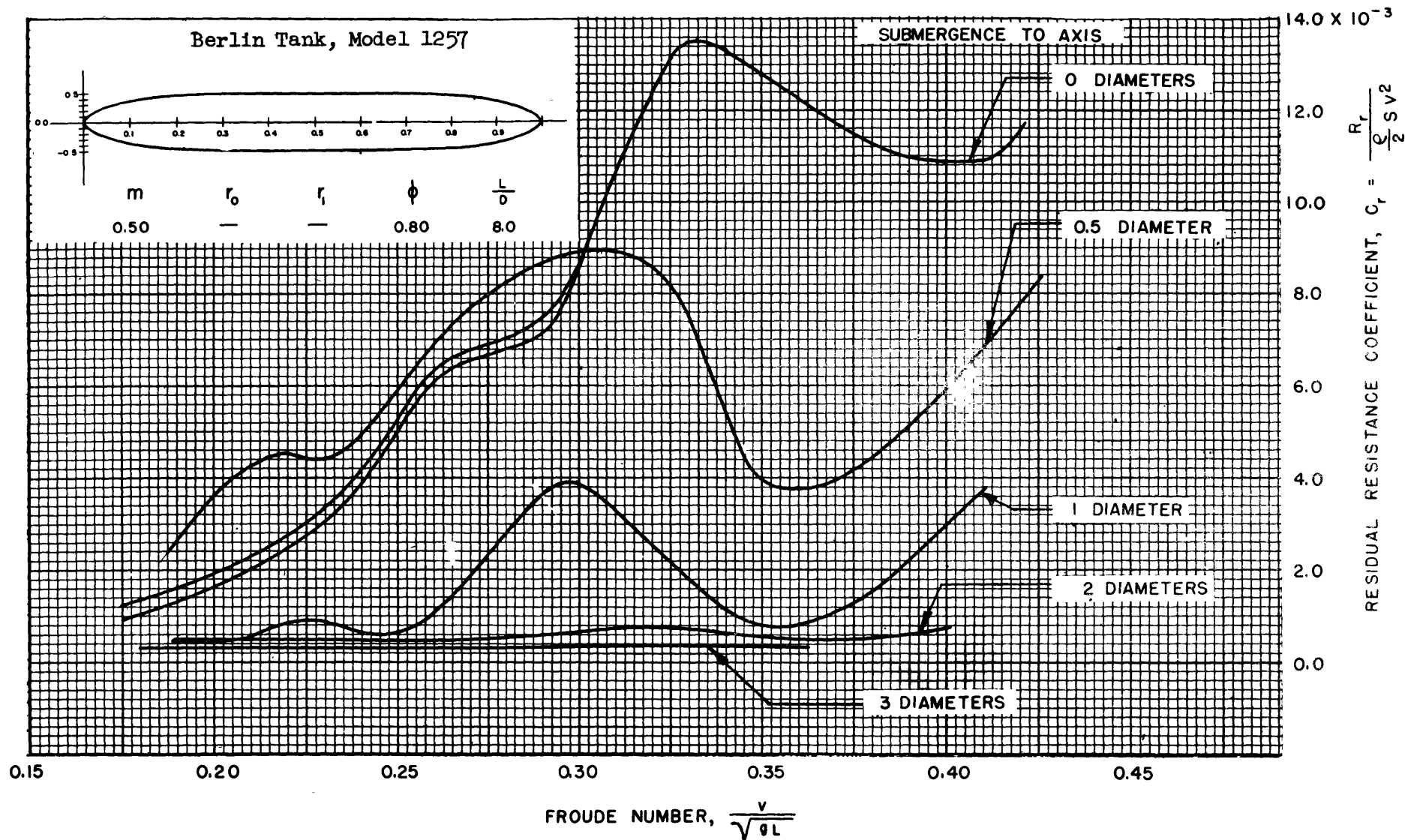


Figure 18 - Residual-Resistance Coefficient versus Froude Number for Model 1257

(The values were obtained by subtracting the Schoenherr frictional-resistance coefficients from the total-resistance coefficients of Figure 9.)

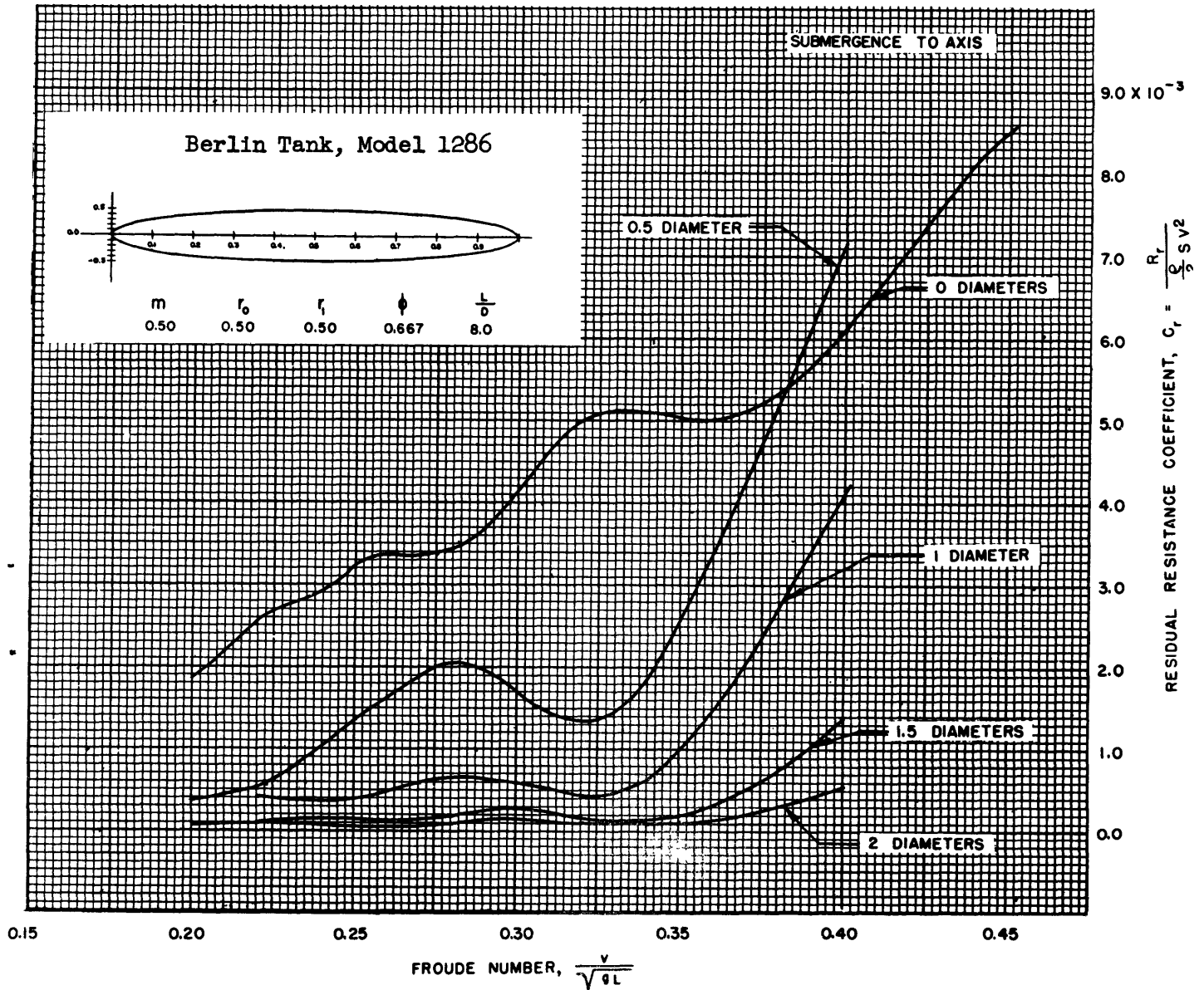


Figure 19 - Residual-Resistance Coefficient versus Froude Number for Model 1286

(The values were obtained by subtracting the Schoenherr frictional-resistance coefficients from the total-resistance coefficients of Figure 10.)

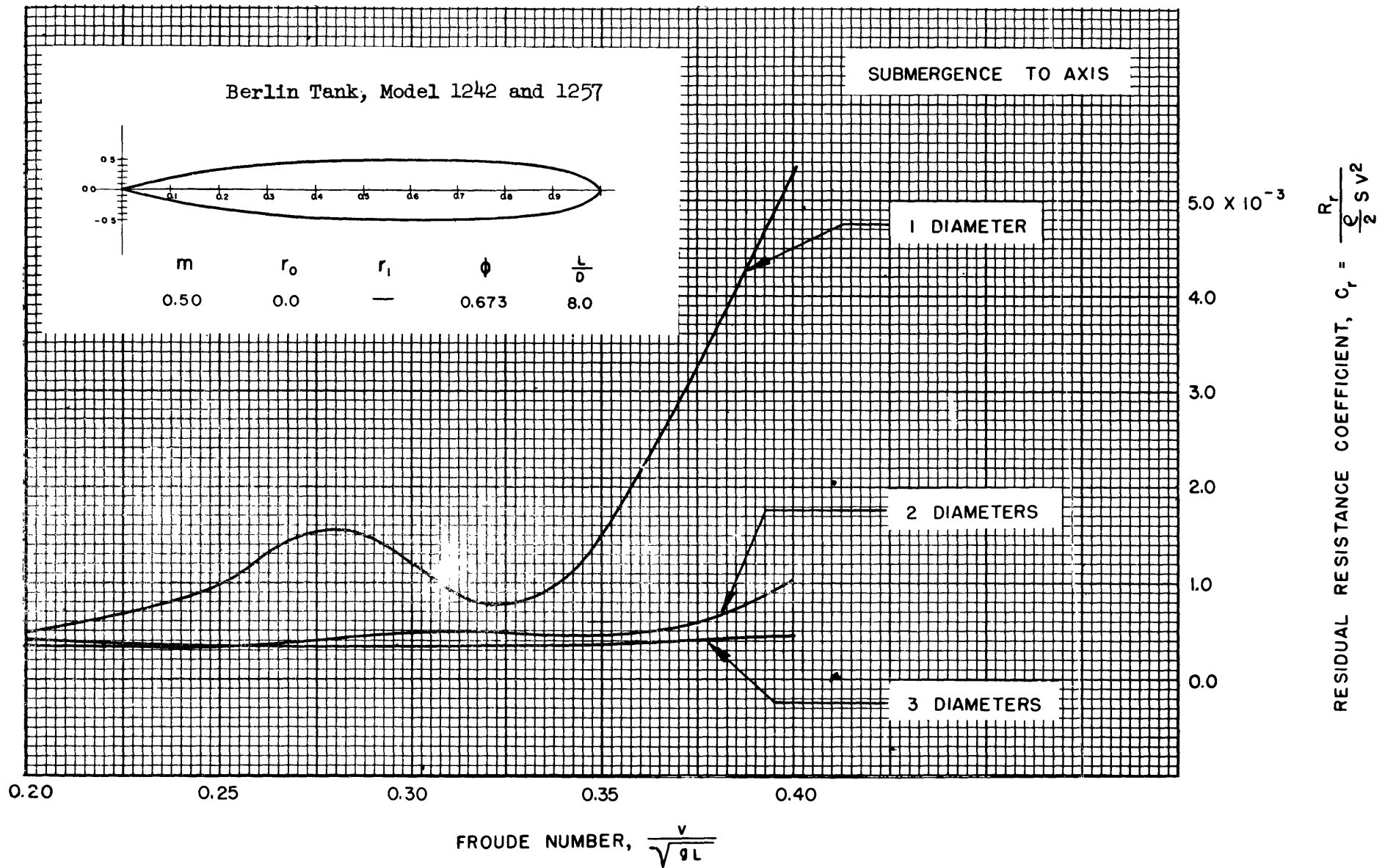


Figure 20 - Residual-Resistance Coefficient versus Froude Number for Models 1242 and 1257

(The values were obtained by subtracting the Schoenherr frictional-resistance coefficients from the total-resistance coefficients of Figure 11.)

